



COB-2021-2071

ASSESSMENT OF THE VOID DISTRIBUTION EFFECT ON THE CONSTITUTIVE BEHAVIOR OF COMPUTATIONALLY HOMOGENIZED POROUS DUCTILE MEDIA

Wanderson Ferreira dos Santos

Ayrton Ribeiro Ferreira

Sergio Persival Baroncini Proença

São Carlos School of Engineering, University of São Paulo. Address: Av. Trab. São Carlense, 400, São Carlos, São Paulo, Brazil
e-mails: wanderson_santos@usp.br; ayrton.ferreira@usp.br; persival@sc.usp.br

Abstract. *The macroscopic constitutive behavior of metals and alloys depends on phenomena originated at the microscale. For example, the effect of porosity can be relevant in the process of ductile failure of these materials. This motivated the development of specialized plastic models to predict the failure of porous ductile solids. In many cases, the yield criteria for porous ductile media adopt the idealized hypothesis of a centered single void in a volume cell. However, in real situations, the voids are randomly distributed within the ductile matrix. In this context, the present paper uses a computational homogenization procedure to study the influence of the void distribution on the homogenized constitutive behavior of porous ductile media. The concept of Representative Volume Element (RVE) is used to model the microstructure of the material. Uniform or periodic boundary conditions are tested in each RVE. The RVE matrix is governed by the von Mises model with perfect elastoplastic behavior. The homogenized constitutive response is obtained by the volume averaging of the microscopic fields provided by the finite element analyses using the ANSYS software. The results show that the void distribution can significantly influence the macroscopic constitutive behavior of porous ductile media.*

Keywords: *metals and alloys, constitutive behavior, computational homogenization, microstructure, distribution of voids.*

1. INTRODUCTION

Multiscale approaches are an interesting alternative for the study of materials with complex behavior. In particular, multiscale strategies based on computational homogenization have been used successfully in the study of heterogeneous media, for example, composites and porous materials. The macroscopic behavior of the material in this case is obtained from analyses carried on a Representative Volume Element (RVE). This technique is typical of works referred to in the literature as FE², that is, with application of finite element discretization in the upper and lower scales.

Feyel (1999) and Feyel and Chaboche (2000) were among some seminal works with the FE² strategy through the simulation of the nonlinear constitutive behavior of composite materials. Terada and Kikuchi (2001) developed a general class of algorithms for the multiscale analysis of the nonlinear behavior of heterogeneous media using variational formulations. Terada *et al.* (2000) carried out simulations of the convergence of multiscale numerical analyses based on computational homogenization. Kouznetsova *et al.* (2001) presented a multiscale strategy with finite element simulations to model heterogeneous materials considering the non-linearity of the material and the hypothesis of large strains. Based on a transition strategy between scales called micro-macro, Miehe and Koch (2002) investigated algorithms to calculate the computationally homogenized constitutive behavior of discretized microstructures in finite elements undergoing small strains.

In a more recent context, Souza Neto and Feijóo (2008) discussed equivalence relationships between spatial and material volume averaging of stress over a RVE in large strain multiscale solid constitutive models. Perić *et al.* (2011) presented a homogenization-based multiscale procedure to describe the macroscopic material response considering nonlinear microstructures undergoing small strains. Blanco *et al.* (2014) showed a unified variational theory for a general class of multiscale models based on the RVE concept. Souza Neto *et al.* (2015) proposed a multiscale theory based on the RVE concept that includes the effect of inertia and body forces. Lopes *et al.* (2017) developed a mixed parallel strategy for solving multiscale problems based on homogenization considering the coupling between scales and the hypothesis of finite strains.

Other works explored computational homogenization approaches to study yield surfaces of porous ductile media. Giusti *et al.* (2009) performed two-dimensional numerical simulations of RVEs with centered voids considering a purely kinematical modelling framework to assess the analytical criterion proposed by Gurson (1977). Fritzen *et al.* (2012) studied the effective material response of ductile metals containing spherical pores by three-dimensional finite elements

simulations. Khdir *et al.* (2015) also used three-dimensional numerical simulations to present overall yield surfaces of random porous media considering the effect of void shape. Carvalho *et al.* (2018) used three-dimensional numerical simulations under the hypothesis of finite strains to obtain yield surfaces of porous media considering centered ellipsoidal voids.

In this context, the present work aims to assess the influence of the void distribution on the computationally homogenized constitutive behavior of porous ductile media. RVEs with different void distributions are studied by two-dimensional numerical simulations by the Finite Element Method (FEM) using the software ANSYS[®] Mechanical, Release 18.0. The RVE matrix is governed by the von Mises model with perfect elastoplastic behavior. The analyses are performed considering the hypothesis of small displacements. In numerical simulations, two boundary conditions are applied in the RVEs: (i) uniform strain boundary condition (UBC); (ii) periodic boundary condition (PBC).

2. HOMOGENIZATION THEORY

Figure 1 shows an illustrative scheme of a multiscale analysis by referring to the macroscale (defined by points \mathbf{y}) and the microscale (defined by points \mathbf{x}). The characteristic dimension of the microscale (l) is much smaller than the characteristic dimension of the macroscale (L), that is, $l \ll L$. On the other hand, the l dimension must be sufficient large to represent the heterogeneities present in the microstructure. In this context, each \mathbf{y} point of the macroscale is modeled in the microscale through the concept of RVE (representative of the microscale). Moreover, the RVE can consider the presence of inclusions and/or voids in the matrix.

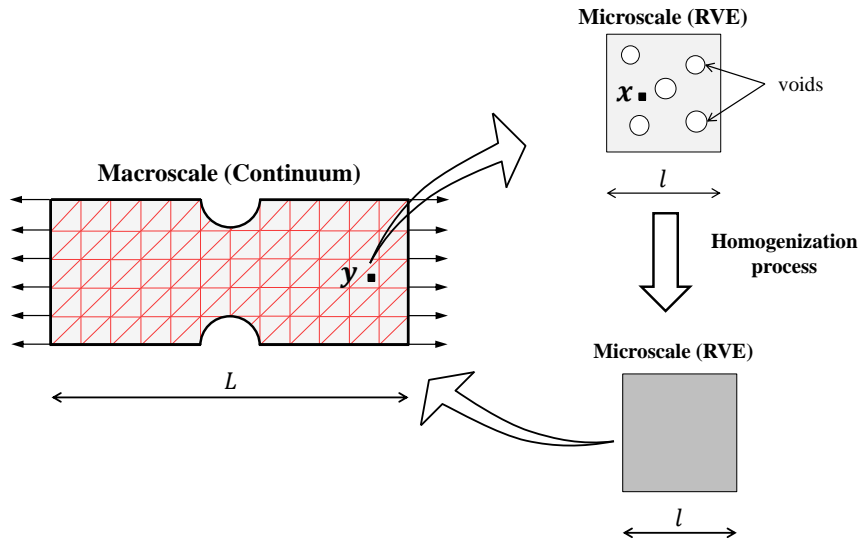


Figure 1. Illustrative scheme of a multiscale modeling considering two scales: (i) macroscale; (ii) microscale.

In the context of multiscale approaches based on homogenization, the macroscopic fields associated with the macroscale (continuum) are obtained by the volume averaging of the microscopic fields (RVE) (Bishop and Hill, 1951):

$$\mathbf{E}(\mathbf{y}) = \frac{1}{V} \int_V \boldsymbol{\varepsilon}(\mathbf{x}) dV = \langle \boldsymbol{\varepsilon}(\mathbf{x}) \rangle \quad (1)$$

$$\boldsymbol{\Sigma}(\mathbf{y}) = \frac{1}{V} \int_V \boldsymbol{\sigma}(\mathbf{x}) dV = \langle \boldsymbol{\sigma}(\mathbf{x}) \rangle \quad (2)$$

where $\boldsymbol{\Sigma}$ and \mathbf{E} are macroscopic stress and strain fields, respectively; $\boldsymbol{\sigma}$ and $\boldsymbol{\varepsilon}$ are microscopic stress and strain fields, respectively; angle brackets ($\langle \rangle$) refer to the volume averaging; V is the total initial volume of the RVE (for small strains). Additionally, Eq. (1) and (2) require both microscopic stress and strain fields to be statically and kinematically admissible, respectively.

The microscale and macroscale domains are associated by the Hill-Mandel Principle of Macro-Homogeneity (see Bishop and Hill (1951) and Mandel (1971)). This principle is based on the equivalence of energy on both scales:

$$\boldsymbol{\Sigma} : \mathbf{E} = \frac{1}{V} \int_V \boldsymbol{\sigma} : \boldsymbol{\varepsilon} dV = \langle \boldsymbol{\sigma} : \boldsymbol{\varepsilon} \rangle \quad (3)$$

The homogenization process involves the resolution of a Boundary Value Problem (BVP) for the RVE. Two commonly used boundary conditions are: (i) Uniform strain boundary condition (UBC); and (ii) Periodic boundary condition (PBC).

The uniform strain boundary condition is given by:

$$\mathbf{u} = \mathbf{E}^* \cdot \mathbf{x} \quad \forall \quad \mathbf{x} \in \partial V \quad (4)$$

with

$$\mathbf{E} = \langle \boldsymbol{\varepsilon} \rangle = \mathbf{E}^*; \quad \boldsymbol{\Sigma} = \langle \boldsymbol{\sigma} \rangle \quad (5)$$

where \mathbf{E} is the macroscopic homogeneous strain tensor applied to the RVE boundary and \mathbf{x} is the coordinate vector. Moreover, an illustrative representation of the deformed RVE considering the UBC is shown in Fig. 2(a).

The periodic boundary condition is given by:

$$\mathbf{u} = \mathbf{E}^* \cdot \mathbf{x} + \tilde{\mathbf{u}} \quad \forall \quad \mathbf{x} \in \partial V \quad (6)$$

with

$$\mathbf{E} = \langle \boldsymbol{\varepsilon} \rangle = \mathbf{E}^*; \quad \boldsymbol{\Sigma} = \langle \boldsymbol{\sigma} \rangle \quad (7)$$

where $\tilde{\mathbf{u}}$ is called periodic fluctuation. In this case, note that: $\langle \tilde{u}_{i,j} \rangle = 0$.

To better understand the periodic boundary condition, the external boundary of the RVE can be regarded as a positive part (Γ^+) and a negative part (Γ^-). In this context, each point \mathbf{x}^+ on Γ^+ has a corresponding point \mathbf{x}^- on Γ^- . Therefore, the displacements of \mathbf{x}^+ are associated with the displacements of \mathbf{x}^- . Figure 2(b) shows a representation of the deformed RVE considering the PBC.

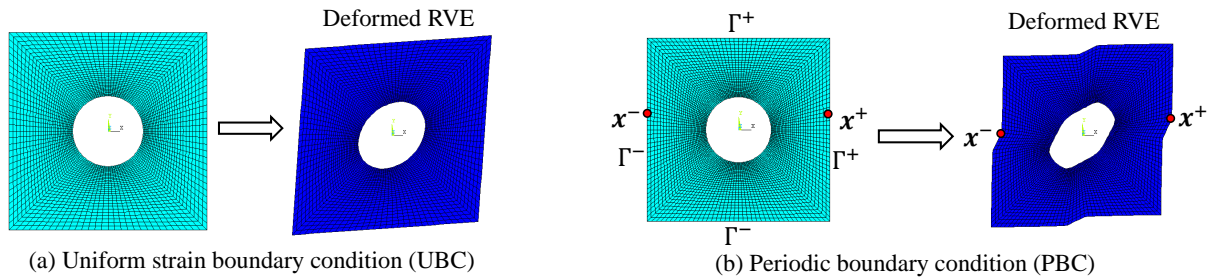


Figure 2. Boundary conditions.

3. METHODOLOGY BASED ON COMPUTATIONAL HOMOGENIZATION TO SIMULATE THE CONSTITUTIVE BEHAVIOR OF POROUS DUCTILE MEDIA

The strategy to study the homogenized constitutive behavior of ductile porous media is presented in this section. Initially, the computational homogenization procedure is shown. Afterwards, the RVE morphologies are presented. Finally, the loading program imposed on the RVEs is described.

3.1 Computational homogenization procedure

In this work, numerical simulations are performed considering the UBC (see Eq. (4)) and the PBC (see Eq. (6)). For both types of boundary conditions, the homogenized strain tensor (\mathbf{E}) results in the macroscopic strain tensor applied in the boundary condition (\mathbf{E}^*), that is, $\mathbf{E} = \mathbf{E}^*$. The homogenized stress tensor is computationally obtained from the microscopic fields calculated by two-dimensional numerical simulations with finite elements:

$$\boldsymbol{\Sigma} = \frac{1}{V} \sum_{i=1}^{N_{elem}} \boldsymbol{\sigma}_i V_i \quad (8)$$

where $\boldsymbol{\Sigma}$ is the computationally homogenized stress tensor; $\boldsymbol{\sigma}_i$ is the average stress in the element i computed at their integration points; V_i is the volume of the element i ; and V is the total initial volume of the RVE.

A preliminary mesh refinement study was carried out to demonstrate the accuracy of the computational homogenization procedure. In particular, the problem of the hollow cylinder submitted to uniform radial external displacement is studied (see Fig. 3).

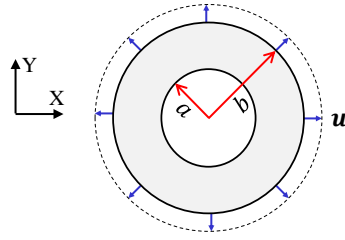


Figure 3. Hollow cylinder submitted to uniform radial external displacement.

The problem in Fig. 3 has an analytical solution for the homogenized mean stress in the XY plane:

$$\Sigma_m^{an} = \frac{2}{\sqrt{3}} \sigma_y \ln \left(\frac{b}{a} \right) \quad (9)$$

where $\Sigma_m^{an} = (\Sigma_x + \Sigma_y)/2$.

Introducing the concept of porosity (f), Eq. (9) can be rewritten as:

$$\Sigma_m^{an} = -\frac{1}{\sqrt{3}} \sigma_y \ln (f) \quad (10)$$

where $f = (a/b)^2$ (i.e., void volume divided by total volume).

The meshes simulated in the refinement study are shown in Fig. 4. Moreover, numerical simulations were performed considering the triangular-shaped element with 6 nodes and 3 integration points.

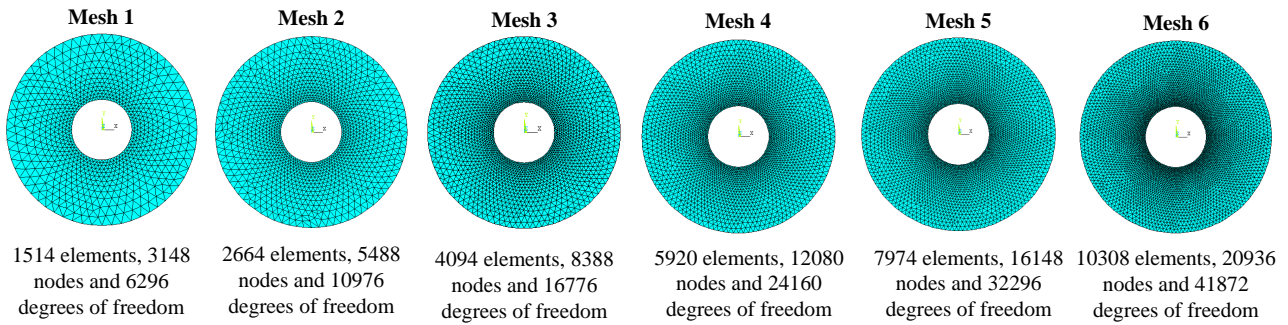


Figure 4. Meshes used in the refinement study.

The hypothesis of plane strain was adopted in the numerical analysis of the hollow cylinder. Furthermore, the UBC was applied to cylindrical RVE considering $\mathbf{E}^* = E_m \mathbf{I}$:

$$\mathbf{u} = \mathbf{E}^* \cdot \mathbf{x} = E_m \mathbf{I} \cdot \mathbf{x} \quad \forall \quad \mathbf{x} \in \partial V \quad (11)$$

where $E_m = \text{Tr}(\mathbf{E})/2$ and \mathbf{I} is the second order identity tensor.

The results of the mesh refinement study are shown in Tab. 1. The relative error (*error*) of the numerical solution (Σ_m^{comp}) compared to the analytical solution (Σ_m^{an}) shows that the computational homogenization procedure provides accurate results.

Table 1. Results of the mesh refinement study considering the triangular-shaped element with 6 nodes.

Elements	Σ_m^{comp} (MPa)	<i>error</i>
1514	319.0900	0.0108%
2664	319.0747	0.0060%
4094	319.0684	0.0040%
5920	319.0640	0.0027%
7974	319.0613	0.0018%
10308	319.0592	0.0012%

3.2 RVEs considering three void distribution configurations

To assess the influence of the void distribution on the homogenized cost behavior of the RVEs, the numerical simulations are performed considering: (i) RVE with 1 centered void; (ii) RVE with 8 voids randomly distributed; (iii) RVE with 16 voids randomly distributed. The meshes used for each RVE are shown in Fig. 5. The ductile matrix is governed by the von Mises model with perfect elastoplastic behavior. The properties of the ductile matrix are defined as: $Y = 200\text{GPa}$ (modulus of elasticity), $\nu = 0.30$ (Poisson's ratio) and $\sigma_0 = 240\text{MPa}$ (microscopic yield stress).

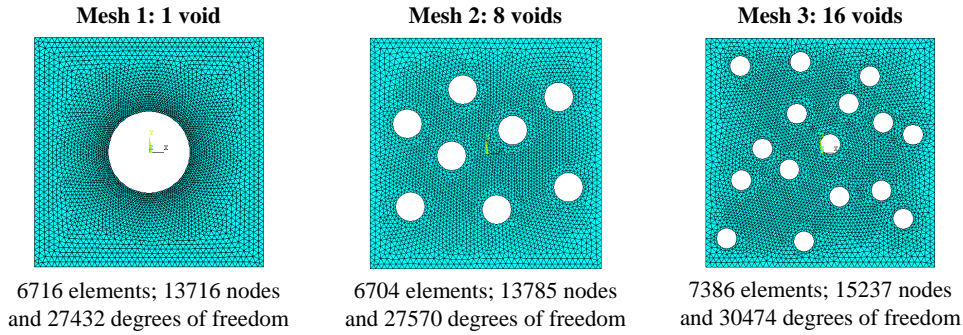


Figure 5. RVEs considering three void distribution configurations.

3.3 Loading programme imposed on the RVEs

The loading programme imposed on the RVEs is based on Giusti *et al.* (2009). In this context, the hypothesis of plane strain is adopted in the numerical analyses of the RVEs. Moreover, the boundary conditions are applied considering the macroscopic strain tensor (\mathbf{E}^*) defined by:

$$\mathbf{E}^* = \frac{\tilde{\mathbf{E}}}{100} \quad (12)$$

with

$$\tilde{\mathbf{E}} = \alpha \begin{bmatrix} \frac{1}{\sqrt{2}} & 0 \\ 0 & \frac{1}{\sqrt{2}} \end{bmatrix} + \sqrt{1 - \alpha^2} \begin{bmatrix} 0 & \frac{1}{\sqrt{2}} \\ \frac{1}{\sqrt{2}} & 0 \end{bmatrix} \quad (13)$$

where $\|\tilde{\mathbf{E}}\| = 1$ and $\alpha \in [0; 1]$. Moreover, $\alpha = 0$ indicates a state of pure shear in the plane and $\alpha = 1$ indicates a state of pure pressure in the plane. Internal values of α in the range $[0; 1]$ correspond to intermediate loading states, that is, with the combination of a volumetric contribution and a distortion contribution.

4. RESULTS AND DISCUSSION

The results of the computationally homogenized constitutive behavior of the RVEs with different void distributions are shown in this section considering three loading situations ($\alpha = 1.0$, $\alpha = 0.5$ and $\alpha = 0.0$).

4.1 Results for $\alpha = 1.0$

Figure 6 shows the homogenized constitutive behavior of the RVEs for $\alpha = 1.0$. Due to the state of pure pressure in the plane, the comparison of results is performed only for $E_x \times \Sigma_x$ and $E_y \times \Sigma_y$. It is clear that the distribution of voids strongly influences the computationally homogenized constitutive responses. The results show that the RVE with a single centered void promotes curves with greater strength. There is also a significant difference between the results of Σ_x and Σ_y in cases with randomly distributed voids. Therefore, the distribution of voids results in a significant anisotropy in the homogenized constitutive behavior of the material. Furthermore, the boundary condition has a significant influence on the homogenized results. Curves with the PBC have less strength compared to the UBC. The distributions of the microscopic normal stresses in the X direction (σ_x) are shown in Fig. 7. Note that the void distribution and the boundary condition influence the microscopic stresses.

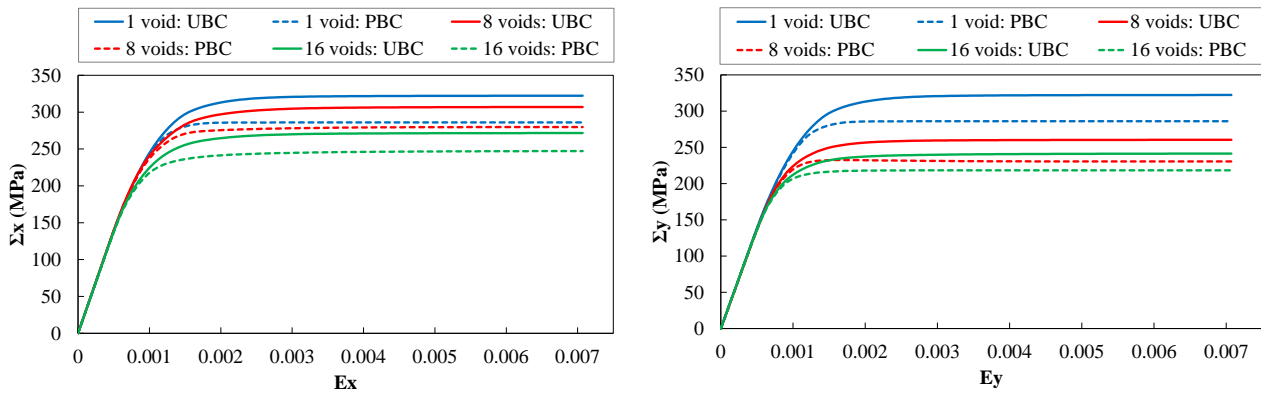


Figure 6. Homogenized constitutive responses ($E_x \times \Sigma_x$ and $E_y \times \Sigma_y$) for $\alpha = 1.0$.

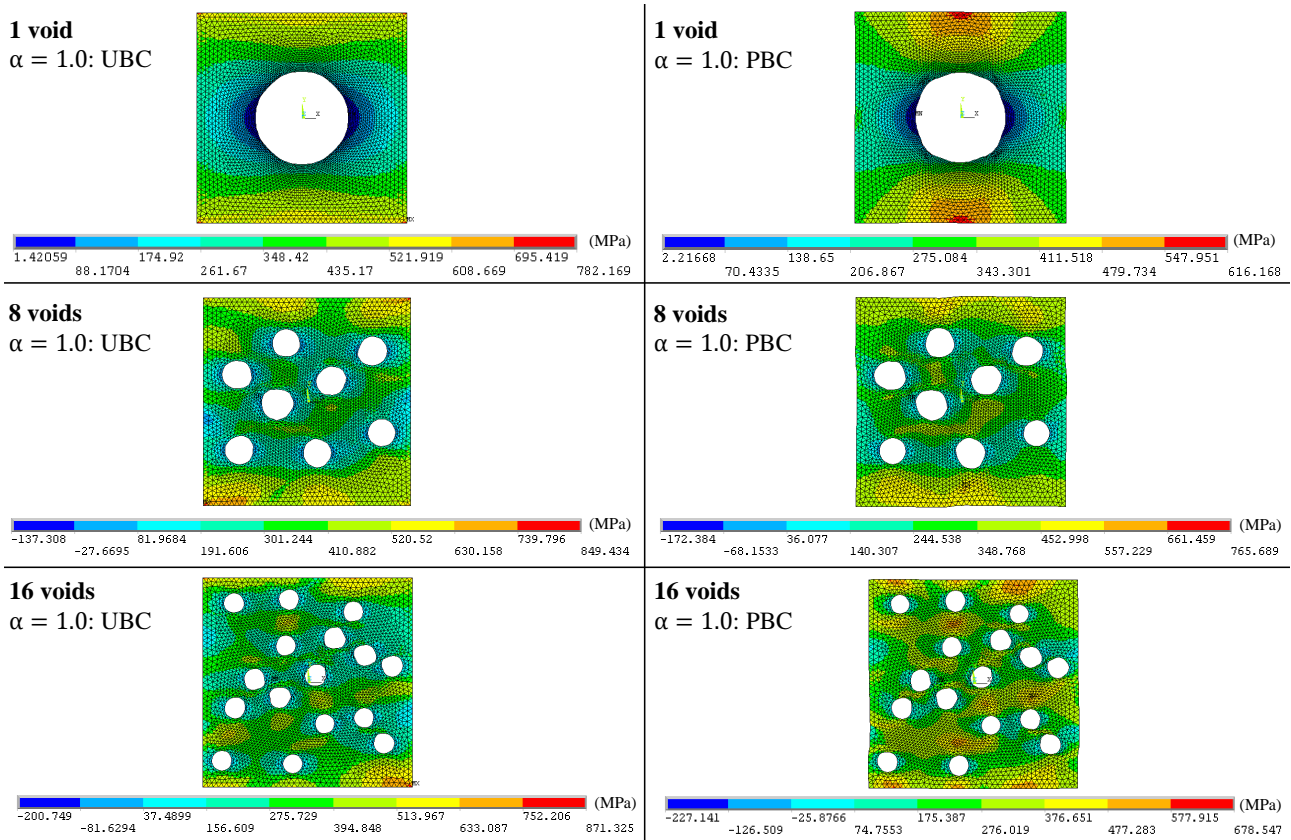


Figure 7. Microscopic normal stress distribution in the X direction (σ_x) for $\alpha = 1.0$.

4.2 Results for $\alpha = 0.5$

Figure 8 presents the homogenized constitutive behavior of the RVEs for $\alpha = 0.5$. The curves $E_x \times \Sigma_x$, $E_y \times \Sigma_y$ and $E_{xy} \times \Sigma_{xy}$ are shown because the applied macroscopic strain tensor corresponds to an intermediate loading state (i.e., combination of pressure in the plane and shear in the plane). The constitutive curve with the tensor norms ($\|\mathbf{E}\| \times \|\Sigma\|$) is also shown in Figure 8. The $\|\mathbf{E}\| \times \|\Sigma\|$ results show curves close to stability (i.e., the maximum strength of the RVE). In the case of the UBC, the RVE with a centered void has greater strength and the RVE with 16 voids has less strength. The differences are greater for $E_x \times \Sigma_x$ and $E_y \times \Sigma_y$ and smaller for $E_{xy} \times \Sigma_{xy}$. Qualitatively, the results obtained for the PBC considering $E_x \times \Sigma_x$ and $E_y \times \Sigma_y$ are analogous. However, the constitutive response $E_{xy} \times \Sigma_{xy}$ considering the PBC shows that the RVE with centered void has less strength and the RVE with 16 voids has greater strength. The curve $E_{xy} \times \Sigma_{xy}$ indicates that the consideration of the PBC results in a strong reduction in the strength of the RVE with a centered void. In quantitative terms, differences in all responses change significantly depending on the stress component under analysis. The distributions of the microscopic stresses are shown in Fig. 9 (considering σ_x) and Fig. 10 (considering σ_{xy}). The microscopic stresses significantly changes with the distribution of voids and also the boundary condition.

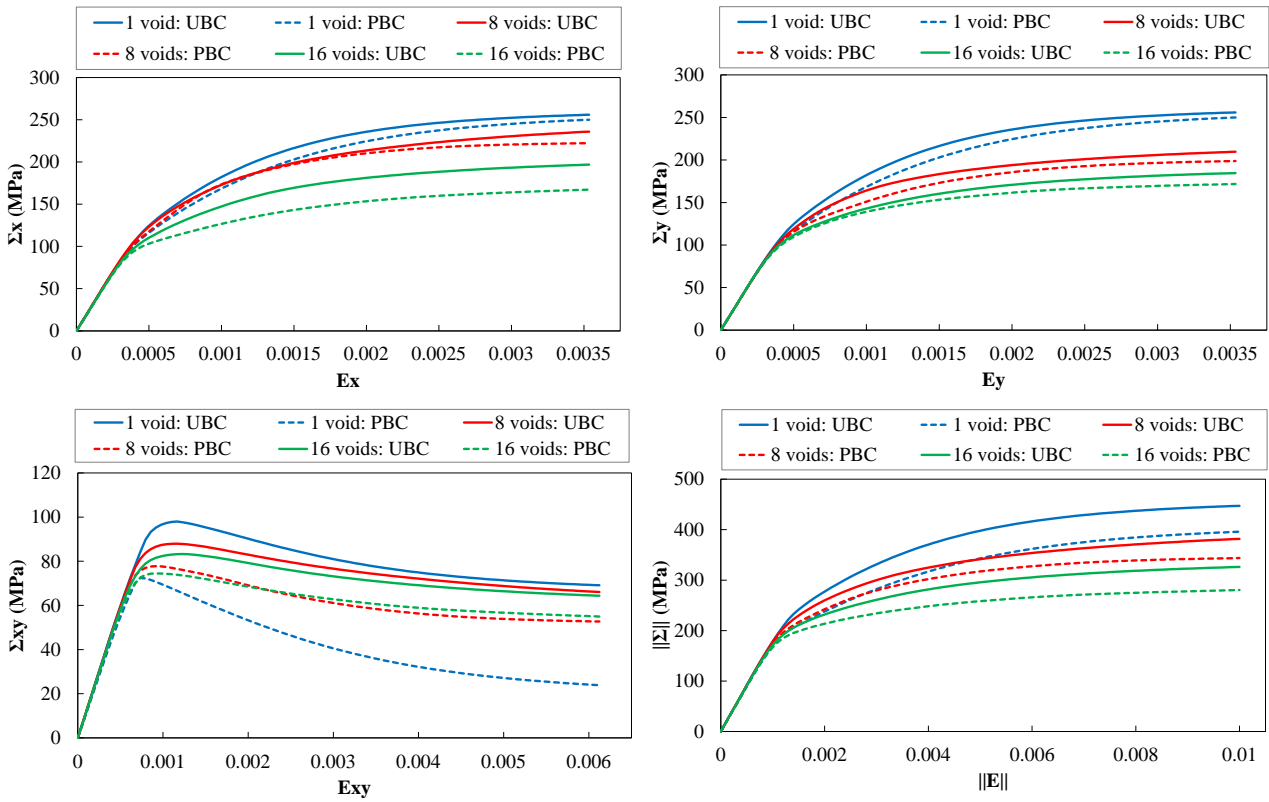


Figure 8. Homogenized constitutive responses ($E_x \times \Sigma_x$, $E_y \times \Sigma_y$, $E_{xy} \times \Sigma_{xy}$ and $\|E\| \times \|\Sigma\|$) for $\alpha = 0.5$.

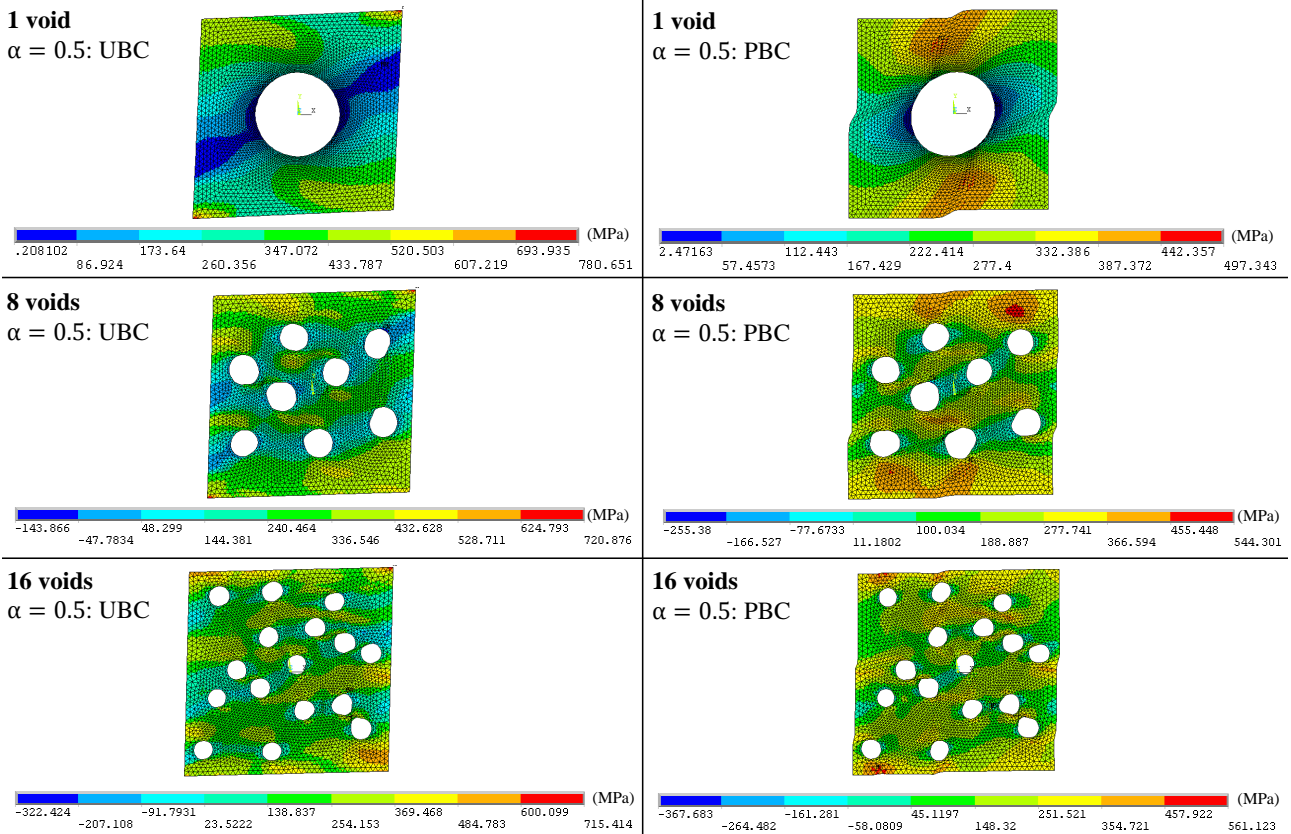


Figure 9. Microscopic normal stress distribution in the X direction (σ_x) for $\alpha = 0.5$.

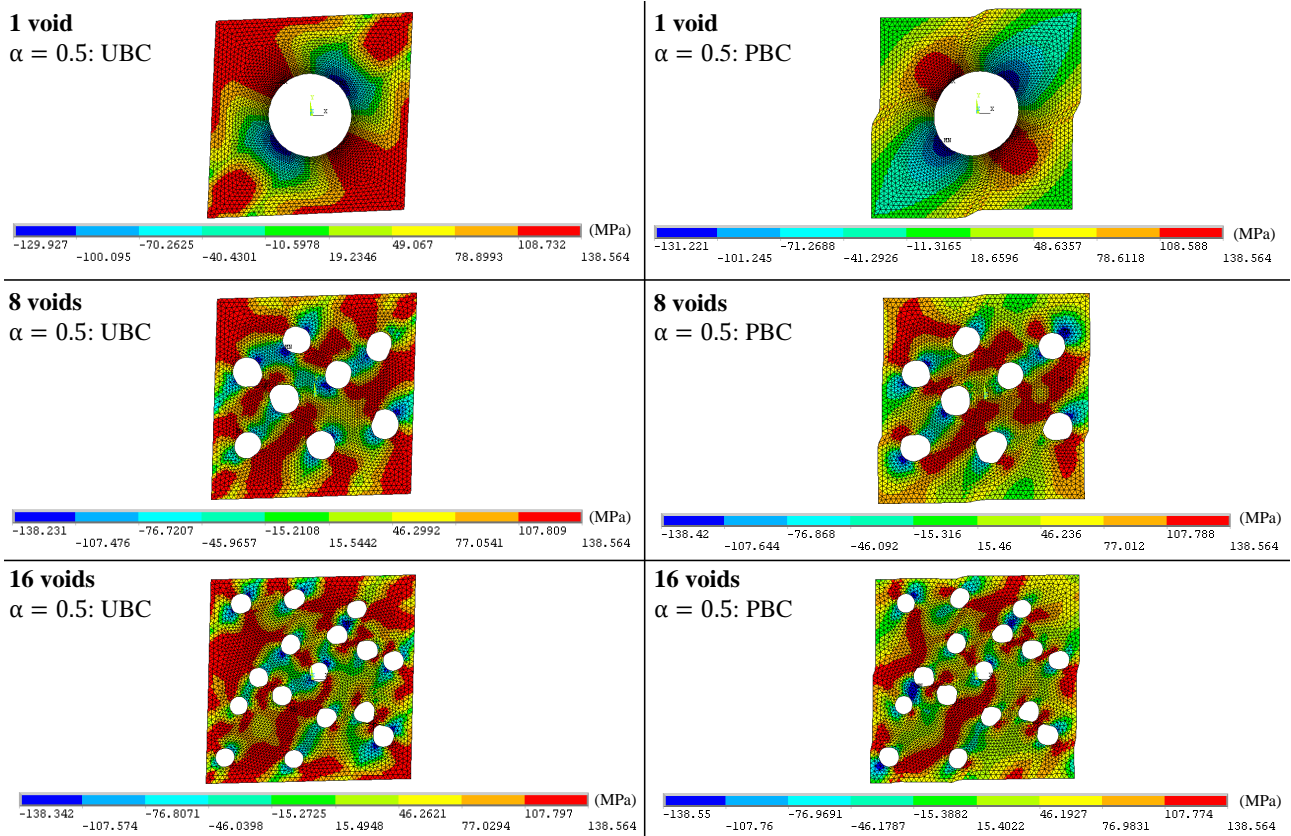


Figure 10. Microscopic shear stress distribution in the XY plane (σ_{xy}) for $\alpha = 0.5$.

4.3 Results for $\alpha = 0.0$

Figure 11 depicts the homogenized constitutive behavior of the RVEs for $\alpha = 0.0$. Only the curve $E_{xy} \times \Sigma_{xy}$ is shown because the applied macroscopic strain state indicates pure shear in the plane. The results of the RVE with centered void have significant differences compared to RVEs with randomly distributed voids. For the UBC, the centered RVE curve has greater strength compared to the other RVE curves with distributed voids (which have close responses). On the other hand, in the case of the PBC, the RVE curve with centered void has less strength when compared to the responses of the other RVEs. The boundary condition has a strong influence on the results, mainly in the RVE with a centered void. This can be explained by the distributions of the microscopic shear stresses in the XY plane (σ_{xy}) shown in Fig. 12. The microscopic stresses strongly depends on the boundary condition and the void distribution. For example, there are concentrations of stresses and displacements in paths that interconnect voids for PBC.

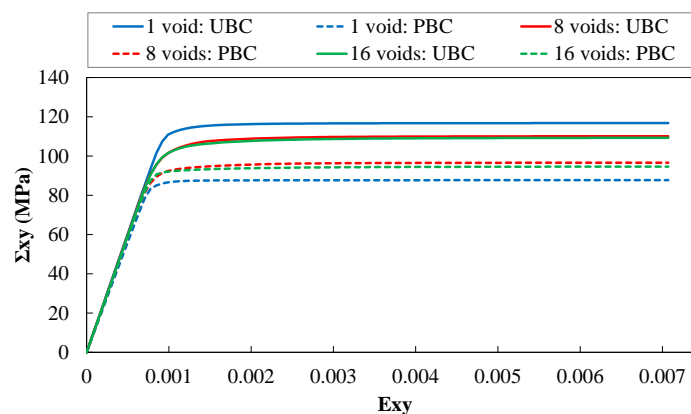


Figure 11. Homogenized constitutive response ($E_{xy} \times \Sigma_{xy}$) for $\alpha = 1.0$.

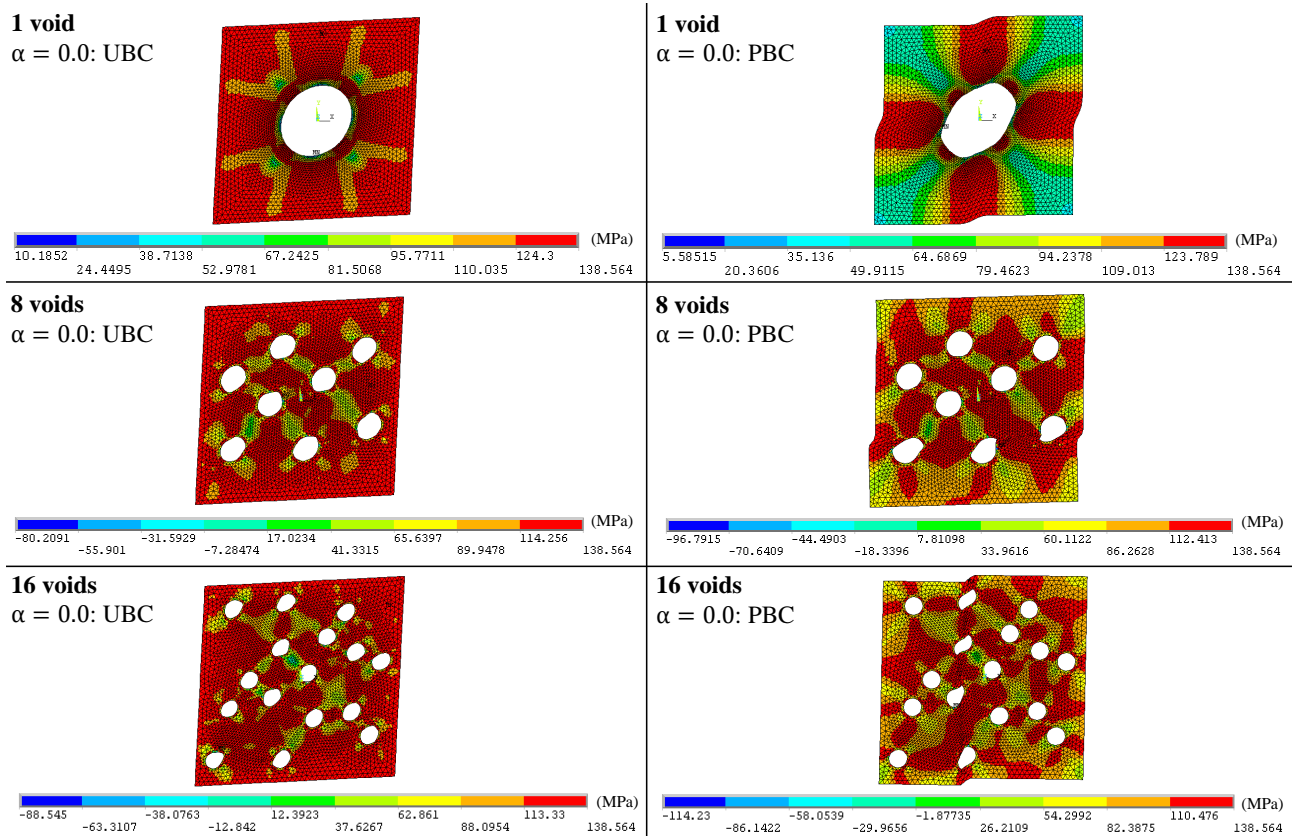


Figure 12. Microscopic shear stress distribution in the XY plane (σ_{xy}) for $\alpha = 0.0$.

5. CONCLUSIONS

This work aimed to assess the influence of the void distribution on the computationally homogenized constitutive behavior of ductile porous media. The results indicate that the void distribution has a strong influence on the homogenized constitutive response of the material. There is sensitive anisotropy in the homogenized response induced by the random distribution of voids. Constitutive curves with PBC have less strength than curves with UBC. In the particular comparison between the responses of the RVEs for the UBC, the RVE with a centered void has homogenized constitutive responses with greater strength in all applied loading cases. Then, the random distribution of the voids promotes results with less strength for UBC. On the other hand, the particular comparison of the RVEs considering the PBC indicates different results for the normal and shear stress components. For the macroscopic normal stress components, the RVE with a centered void has greater strength considering the PBC. However, for the macroscopic shear stress component, the RVE with a centered void has less strength considering the PBC. Then, the boundary condition also plays an important role in the results. The above conclusions show that the constitutive behavior of ductile porous media is complex and the computational homogenization allowed to capture important information observed at the microscale. Therefore, the results of this work contribute to a more realistic computational modeling of the macroscopic constitutive behavior of metals and alloys considering random void distribution.

6. ACKNOWLEDGEMENTS

The authors would like to gratefully acknowledge Conselho Nacional de Desenvolvimento Científico e Tecnológico - Brasil (CNPq) and Coordenação de Aperfeiçoamento de Pessoal de Nível Superior - Brasil (CAPES) for the research grants. This study was also financed in part by the Coordenação de Aperfeiçoamento de Pessoal de Nível Superior - Brasil (CAPES) - Finance Code 001.

7. REFERENCES

- Bishop, J.F.W. and Hill, R., 1951. "XLVI. A theory of the plastic distortion of a polycrystalline aggregate under combined stresses." *Philosophical Magazine Series 5*, Vol. 42, pp. 414–427.
- Blanco, P.J., Sánchez, P.J., Souza Neto, E.A.d. and Feijóo, R.A., 2014. "Variational foundations and generalized unified theory of rve-based multiscale models". *Archives of Computational Methods in Engineering*, Vol. 23, pp. 191–253.

- Carvalho, R.P., Lopes, I.A.R. and Pires, F.M.A., 2018. "Prediction of the yielding behaviour of ductile porous materials through computational homogenization". *Engineering Computations*, Vol. 35, pp. 604–621.
- Feyel, F., 1999. "Multiscale FE2 elastoviscoplastic analysis of composite structures". *Computational Materials Science*, Vol. 16, pp. 0–354.
- Feyel, F. and Chaboche, J.L., 2000. "FE2 multiscale approach for modelling the elastoviscoplastic behaviour of long fibre sic/ti composite materials". *Computer Methods in Applied Mechanics and Engineering*, Vol. 183, pp. 309–330.
- Fritzen, F., Forest, S., Böhlke, T., Kondo, D. and Kanit, T., 2012. "Computational homogenization of elasto-plastic porous metals". *International Journal of Plasticity*, Vol. 29, pp. 102–119.
- Giusti, S., Blanco, P., Souza Neto, E.A. and Feijóo, R.A., 2009. "An assessment of the gurson yield criterion by a computational multi-scale approach". *Engineering Computations*, Vol. 26, pp. 281–301.
- Gurson, A.L., 1977. "Continuum theory of ductile rupture by void nucleation and growth: Part i—yield criteria and flow rules for porous ductile media". *Journal of Engineering Materials and Technology*, Vol. 99, No. 1, pp. 2–15.
- Khdir, Y.K., Kanit, T., Zaïri, F. and Naït-Abdelaziz, M., 2015. "A computational homogenization of random porous media: Effect of void shape and void content on the overall yield surface". *European Journal of Mechanics - A/Solids*, Vol. 49, pp. 137–145.
- Kouznetsova, V., Brekelmans, W.A.M. and Baaijens, F.P.T., 2001. "An approach to micro-macro modeling of heterogeneous materials". *Computational Mechanics*, Vol. 27, pp. 37–48.
- Lopes, I.A.R., Pires, F.M.A. and Reis, F.J.P., 2017. "A mixed parallel strategy for the solution of coupled multi-scale problems at finite strains". *Computational Mechanics*.
- Mandel, J., 1971. *Plasticité classique et viscoplasticité*. Springer-Verlag, Udine, Italy.
- Miehe, C. and Koch, A., 2002. "Computational micro-to-macro transitions of discretized microstructures undergoing small strains". *Archive of Applied Mechanics*, Vol. 72, pp. 300–317.
- Perić, D., Souza Neto, E.A., Feijóo, R.A., Partovi, M. and Molina, A.J.C., 2011. "On micro-to-macro transitions for multi-scale analysis of non-linear heterogeneous materials: unified variational basis and finite element implementation". *International Journal for Numerical Methods in Engineering*, Vol. 87, pp. 149–170.
- Souza Neto, E.A., Blanco, P.J., Sánchez, P.J. and Feijóo, R.A., 2015. "An rve-based multiscale theory of solids with micro-scale inertia and body force effects". *Mechanics of Materials*, Vol. 80, pp. 136–144.
- Souza Neto, E.A. and Feijóo, R.A., 2008. "On the equivalence between spatial and material volume averaging of stress in large strain multi-scale solid constitutive models". *Mechanics of Materials*, Vol. 40, pp. 803–811.
- Terada, K., Hori, M., Kyoya, T. and Kikuchi, N., 2000. "Simulation of the multi-scale convergence in computational homogenization approaches". *International Journal of Solids and Structures*, Vol. 37, pp. 2285–2311.
- Terada, K. and Kikuchi, N., 2001. "A class of general algorithms for multi-scale analyses of heterogeneous media". *Computer Methods in Applied Mechanics and Engineering*, Vol. 190, pp. 5427–5464.

8. RESPONSIBILITY NOTICE

The authors are solely responsible for the printed material included in this paper.